

# CUTTING FORCE MODELLING IN ORTHOGONAL TURNING OF C/PEEK AND C/PA12

JAROSLAV KOVALCIK, PETR MASEK, PAVEL ZEMAN

Department of Production Machines and Equipment (RCMT),  
Faculty of Mechanical Engineering, Czech Technical  
University in Prague, Czech Republic

DOI: 10.17973/MMSJ.2022\_11\_2022131

e-mail: [j.kovalcik@rcmt.cvut.cz](mailto:j.kovalcik@rcmt.cvut.cz)

This article focuses on cutting force modelling in the orthogonal turning of two commonly used types of fibre-reinforced plastic materials. Uncoated cutting tool inserts made of sintered carbide and with different rake angles were used for the designed experiments. In addition to the different rake angles in the experiments, there were also different feeds per revolution and cutting speeds. It was found that the effect of the feed per revolution and the rake angle on the cutting force is statistically significant for both materials. On the other hand, the effect of the cutting speed on the cutting force is statistically insignificant. Therefore, a mathematical model of the cutting force with the impact of the feed per revolution as well as the rake angle was developed and based on the experimental data all constants needed for the proposed mathematical model were found. Based on the comparison of the calculated and experimental cutting forces it was found that there was no statistically significant difference between them, and the proposed model can be therefore considered sufficiently accurate in the given range of the cutting conditions.

## KEYWORDS

Turning, Fibre-reinforced plastics, Cutting force, Specific cutting force, C/PEEK, C/PA12

## 1 INTRODUCTION

Fibre-reinforced plastics (FRP) belong to a group of materials with a favourable strength-to-weight ratio. The strength of the material is provided by fibres with a thickness of several microns. These fibres can be arranged in the polymer matrix in different ways in terms of length, volume ratio and orientation in the matrix. The matrix serves as the bulk filler of the material. It transfers the load to the fibres, fixes the fibres in the desired position and protects them from the environment. Polymer matrices are either thermoset or thermoplastic; each type exhibits different heat behaviour. The fibres can be carbon, glass, natural or polymer. The choice of matrix, fibres and their placement affect both the composite properties and machinability [Davim 2010].

Composite machining is challenging in terms of the high abrasion of the fibres, low heat conduction of heat and a low melting point of the soft matrix as well as reaching the high quality of machining surface. The cutting forces and temperature in the cut affect the quality of the machined surface in terms of delamination. Temperature in the cut was described in previous study [Masek 2021]. Cutting forces are due to the interaction between the cutting tool and the workpiece. These forces are sensitive to the macro and micro geometric cutting tool features and wear changes to these features. However, the forces are also sensitive to cutting conditions and workpiece material properties or internal defects in the workpiece material.

Composite materials are inherently inhomogeneous. Santhanakrishnan noted the effect of cutting tool material on the magnitude of forces in turning CFRP [Santhanakrishnan 1992]. He attributed this phenomenon to the different thermal conductivity of the type of carbide used. Chang also observed these differences in cutting forces for carbide types K and P; see [Chang 2006]. He also found the effect of the chamfered cutting edge on the forces and temperatures. Davim presented a significant reduction in all force components when machining PA66 with 30% glass fibre-reinforced polymer (GFRP) compared to PA66 without reinforcement, probably due to the ductility of PA66 [Davim 2009]. He also found that the cutting force components are reduced by decreasing the cutting tool rake angle due to the smaller length of chip contact with the cutting tool rake face. In an earlier study, Davim observed higher forces for PA6 than for 30% glass fibre-reinforced PA66, with PA6 having up to 2 times higher tensile strength and higher modulus [Davim 2007a]. İşik also documented increasing forces for glass fibre composite E [İşik 2011]. In this study, the nose radius also increased the forces, but only slightly. Kumar investigated a hand-laid bi-directional carbon fiber reinforced CFRP composite in underhole turning [Kumar 2014]. In contrast to the previously mentioned study, cutting speed increased the cutting force and feed rate decreased the cutting force. This is also contrary to the machining theory where the cutting force increases with chip thickness. David performed machining of GFRP with 65% glass content [Davim 2007b]. He found that cutting speed was of little significance to the specific cutting force, but that feed rate had a very significant effect. Roy presented turning CFRP at high cutting speeds of up to 346 m/min [Roy 2014]. The force components decreased with cutting speed. Sauer explained the increase in cutting force with feed rate and depth of cut by the larger number of machined fibres when turning CFRP, see [Sauer 2020]. However, the matrix also contributed to the increase in force.

There is a very limited number of publications on force modelling in FRP turning. However, modelling cutting forces are important in terms of optimizing cutting tool performance, process parameters or cost reduction. In the case of inhomogeneous composite materials, force models can be quite complicated when they describe the breakage of the fibres and the effect of the matrix under oblique cutting. The first level of simplification is the necessity of describing the force model in orthogonal machining. Here the forces action can be solved in the plane. Chen presented a sophisticated micromechanical model of cutting forces for orthogonal machining (shaping) with a relative error of up to 22 % [Chen 2017]. Takeyama's model described a macro view of fibre orientation in FRP where the elastic interaction between fibres and matrix was neglected [Takeyama 1988]. A different approach to modelling forces is offered by mechanistic models, which are based on the similarity of the measured trend of a data set to a known mathematical function. This type of model was used, for example, by Wang for cutting tool geometry [Wang 1995]. Numerical methods use finite element methods, which have been used, for example, by Abena [Abena 2015] and Mahdi [Mahdi 2001]. Oblique turning is a three-dimensional problem for solving force models and has been addressed in a limited number of papers. Ntziantzias used the Kinzle-Victor mechanistic model to predict cutting forces in GFRP [Ntziantzias 2011]. The presented model fits the measured data with an average error of 6.5%. Özden compared an artificial neural network (ANN) and adaptive-neural fuzzy inference system (ANFIS) for a turning force model of C/PEEK composite with coefficients of determination ( $R^2$ ) of 93 % and 98 %, respectively [Özden 2021]. Kumar used a regression model for

the force components during turning of UD-GFRP with  $R^2$  above 96% [Kumar 2015].

Based on the literature review, a mechanistic model was selected for modelling of cutting forces. The accuracy of the selected method is adequate for predicting the cutting force. The model will be applied to orthogonal turning. Two widely used materials with different properties were chosen from thermoplastic composites – C/PA12 and C/PEEK.

A disk embedding experiment was designed to find the specific cutting force coefficients. Disc turning simulates the indentation operation, which is very effective in machining the ends of composite tubes to specific dimensions.

## 2 DESIGN OF EXPERIMENTS

### 2.1 Machine tool and measuring devices

The experiments of orthogonal turning were carried out on an SP 430 SY 2 1100 CNC turning machine centre (Kovosvit MAS company); see Figure 1. The maximum spindle power of the S1 mode was 28 kW, the maximum torque of the S1 mode was 1403 Nm, the nominal speed of the machine was 141 rpm and the maximum speed was 3150 rpm. On this CNC machine centre, a 9119AA1 piezoelectric dynamometer (KISTLER company) was clamped. A 5167A laboratory charge amplifier with integrated data acquisition and a laptop with Dynoware software were used for cutting force measurement and evaluation

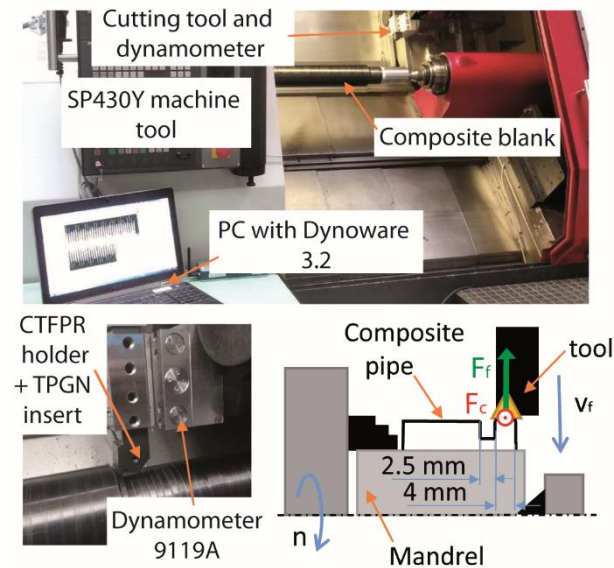


Figure 1. Experimental setup of the CNC turning machine

### 2.2 Cutting tool

A cutting tool holder with a cutting edge angle ( $\kappa_r$ ) of  $90^\circ$ , with three types of cutting tool inserts of a triangular shape, were used. All three inserts were made of sintered carbide and had no coating. The standard cemented carbide for non-ferrous materials was chosen for the experimental investigation. The chemical composition of the cemented carbide in volume percentages was: WC (92 %), NbC + TaC (2 %) and Co (6 %). The real geometry of the cutting tool inserts was measured with an Alicona InfiniteFocus G5 (Alicona Imaging GmbH) device; see Table 1. As can be seen, the real rake angles of the cutting tool inserts are:  $0^\circ$  (Sample A),  $10^\circ$  (Sample B) and  $20^\circ$  (Sample C). The tool geometry was manufactured by laser technology on the standard TPGN insert. When the cutting tool inserts are clamped in the cutting tool holder, the resulting rake angles are:  $5^\circ$ ,  $15^\circ$  and  $25^\circ$ . The change of the rake angles was caused by rake angle of the tool holder bed, which was  $5^\circ$ .

Parameter	Symbol	Unit	Cutting tool insert		
			A	B	C
Cutting edge radius	$r$	$\mu\text{m}$	3.96	3.28	2.10
Nose radius	$r_\epsilon$	mm	0.8	0.8	0.8
Surface roughness	$R_a$	$\mu\text{m}$	0.42	0.45	0.36
Clearance angle	$\alpha_o$	$^\circ$	11	11	11
Wedge angle	$\beta_o$	$^\circ$	79	69	59
Rake angle	$\gamma_o$	$^\circ$	0	10	20

Table 1. Real cutting tool geometry of the cutting tool inserts

### 2.3 Workpiece

The experiments were performed on two types of composite materials with a thermoplastic matrix and carbon fibres, marked as C/PEEK and C/PA12. Both composites had the same volume of identical reinforcement (T700 reinforcement). The PEEK-type matrix is a high-performance composite with high tensile strength and heat resistance. On the other hand, PA12 is a common industrial type of matrix with lower mechanical and physical properties. Differences between matrices lead to significant machinability changes which are manifested by cutting force change. The properties of both materials are shown in Table 2. The composite materials were wound on a rod in tape form.

Property	Unit	Composite material	
		C/PA12	C/PEEK
Reinforcement volume	%	55	
Layer angle of winding on tube	$^\circ$	$\pm 65$	
Tensile strength	MPa	1650	4650
Short beam shear strength	MPa	40	90
Adhesive fracture energy	$\text{kJ/m}^2$	0.83	1.32
Longitudinal elastic modulus	MPa	133	142

Table 2. Material and mechanical properties of both composite materials

### 2.4 Proposed design of experiments

The design of the experiments assumed a constant chip width, i.e. 4 mm, which is the thickness of a disc. The main focus of all cutting conditions was the feed per revolution, which had five levels ranging from 0.05 to 0.30 mm. To see the impact of the cutting speed on the cutting force, two cutting speeds were used: 150 m/min and 300 m/min. All of these experiments were performed for a cutting tool with three different rake angles:  $5^\circ$ ,  $15^\circ$  and  $25^\circ$ . Table 3 summarizes the design of the experiments for both workpiece materials.

Parameter	Symbol	Unit	Levels				
			1	2	3	4	5
Feed per rev.	$f$	mm	0.05	0.1	0.15	0.2	0.3
Rake angle	$\gamma_o$	$^\circ$	5	15	25		
Cutting speed	$v_c$	m/min	150	300			

Table 3. Design of experiments

There were 30 experiments for each workpiece material. Each experiment had three repetitions. The experiments were performed randomly to exclude any measurement errors.

## 3 RESULTS AND DISCUSSION

### 3.1 Force measurements

The force measurements revealed the strong influence of the feed force ( $F_f$ ) on the composite ply organization; see Figure 2.

The passive force ( $F_p$ ) was almost zero in all measurements and cutting conditions had no effect on it.

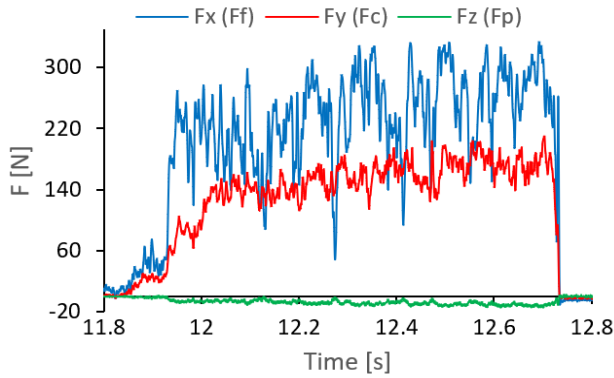


Figure 2. An example of force measurement for C/PEEK ( $v_c = 300$  m/min,  $f = 0.3$  mm,  $\gamma_o = 5^\circ$ )

The passing of the cutting tool through the ply caused a strong amplitude and oscillation of the feed force, where the peaks of minimum force represented the number of plies in the winding. This phenomenon was caused by decreasing in specific cutting force between plies. Most likely, this decrease is affected by insufficient bonding of prepregs. This force was burdened by a higher measurement error due to this phenomenon. More extensive force peaks were observed for C/PEEK than for C/PA12. A reason for this consists in the higher mechanical properties of C/PEEK partially because the higher mechanical properties of the composite ply led to a bigger drop of force between plies. The amplitude of peaks was strongly dependent on the feed per revolution for the cutting force as well as the feed force. This amplitude increased with the feed per revolution due to higher deformation in each ply, whereas between plies the cutting tool goes through with minimal resistance of machined material. The oscillation of  $F_f$  seems to be affected by the rake angle and it was found that the higher the rake angle, the higher the oscillation.

On the other hand, the cutting force was affected by the force drop between plies only slightly. This force component could be predicted more simply and with greater reliability.

Figure 3 as well as the ANOVA test, see Table 3 and Table 4, show the impact of three separate factors on the cutting force, namely feed per revolution, cutting speed and rake angle. As can be seen, the cutting force is strongly affected by the feed per revolution and as it increases the cutting force also increases. Another factor that strongly affects the cutting force is the rake angle. As it increases the cutting force decreases. It was also observed that the composite material C/PEEK is more sensitive to rake angle changes. On the other hand, the cutting speed does not have a statistically significant effect on the cutting force. This behaviour is consistent with the machining theory of metals.

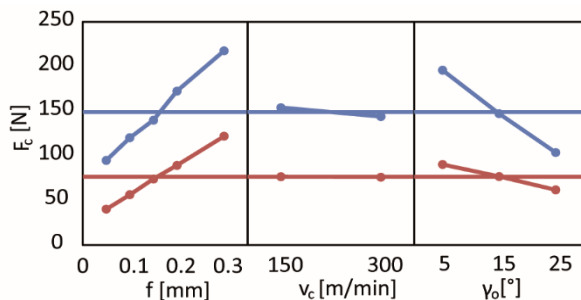


Figure 3. The influence of different factors on the cutting force (C/PEEK – blue curve, C/PA12 – red curve)

Source	DF	Adj SS	Adj MS	F-Value	P-Value
--------	----	--------	--------	---------	---------

$\gamma_o$	2	4039.0	2019.51	132.65	0.000
$v_c$	1	1.6	1.56	0.10	0.752
$f$	4	23698.0	5924.50	389.15	0.000
Error	22	334.9	15.22		
Total	29	28073.5			

Table 4. Analysis of variance for C/PA12

Source	DF	Adj SS	Adj MS	F-Value	P-Value
$\gamma_o$	2	42564	21282.0	38.50	0.000
$v_c$	1	766	766.2	1.39	0.252
$f$	4	54604	13651.0	24.69	0.000
Error	22	12162	552.8		
Total	29	110097			

Table 5. Analysis of variance for C/PEEK

### 3.2 Cutting force modelling

Based on the review, a modelling method built on the product of the specific cutting force and cutting area, where the basic form of the specific cutting force is based only on the effect of the undeformed chip thickness, was selected; see equation (1).

$$\left. \begin{aligned} k_c &= k_{c_{1.1}} \cdot h_D^{-m_c} \\ A_D &= h_D \cdot b_D \end{aligned} \right\} F_c = k_c \cdot A_D = k_{c_{1.1}} \cdot h_D^{1-m_c} \cdot b_D \quad (1)$$

where:

$A_D$  [mm<sup>2</sup>] ... undeformed chip area

$b_D$  [mm] ... undeformed chip width

$F_c$  [N] ... cutting force

$h_D$  [mm] ... undeformed chip thickness

$k_{c_{1.1}}$  [N/mm<sup>2</sup>] ... specific cutting force for a cutting area of 1 mm<sup>2</sup>

$k_c$  [N/mm<sup>2</sup>] ... specific cutting force for a particular undeformed chip thickness

$m_c$  [-] ... constant that determines the effect of the undeformed chip thickness on the specific cutting force

In equation (1), there are two material constants ( $k_{c_{1.1}}$ ,  $m_c$ ) that have to be determined for both of the proposed workpiece materials.

The analysis of variance of both composite materials shows that the rake angle has a significant effect on the cutting force; see Table 4 and Table 5. Neglecting this factor would lead to inaccuracy in the prediction. In Figure 3, the rake angle effect on the cutting force is linear and thus it is possible to use the equation used by Degner, Kovalčík and Tschatsch [Degner 2015, Kovalčík 2020, Tschatsch 2009], which supplements the basic equation of the specific cutting force by the rake angle correction factor ( $K_{\gamma_o}$ ). This correction factor is calculated according to equation (2). The specific cutting force is then calculated according to equation (3) and the cutting force by using equation (4).

$$K_{\gamma_o} = 1 - X \cdot (\gamma_{o_1} - \gamma_{o_0}) \quad (2)$$

$$k_c = k_{c_{1.1}} \cdot h_D^{-m_c} \cdot [1 - X \cdot (\gamma_{o_1} - \gamma_{o_0})] \quad (3)$$

$$F_c = k_{c_{1.1}} \cdot h_D^{1-m_c} \cdot [1 - X \cdot (\gamma_{o_1} - \gamma_{o_0})] \cdot b_D \quad (4)$$

where:

$\gamma_{o_0}$  [°] ... rake angle of the cutting tool for which the material constants are obtained

$\gamma_{o_1}$  [°] ... rake angle of the cutting tool for which the cutting force is currently calculated

$K_{\gamma_o}$  [-] ... rake angle correction factor

$X$  [-] ... constant used to calculate the rake angle correction factor

Equation (3) contains the constant  $X$ , which also has to be determined for each workpiece material. In this equation two rake angles can be seen. These rake angles are the resulting rake angles when the inserts are clamped in the cutting tool holder. Equation (3) was used to find all of the unknown constants ( $k_{c1.1}$ ,  $m_c$ ,  $X$ ). In our case, the undeformed chip thickness is equal to the feed per revolution. As for the rake angle  $\gamma_{o0}$ ,  $5^\circ$  was chosen from the available rake angles ( $5^\circ$ ,  $15^\circ$ ,  $25^\circ$ ). All three unknown constants were obtained by using Minitab software and are shown in Table 6.

Material	Parameter		
	$k_{c1.1} \left[ \frac{N}{mm^2} \right]$	$m_c [-]$	$X [-]$
C/PA12	70	0.419	0.019
C/PEEK	108	0.551	0.018

**Table 6.** Constants obtained for each composite material

The effect of undeformed chip thickness on the specific cutting force change, characterized by the constant  $m_c$ , is greater for C/PEEK than for C/PA12. The rake angle effect on the specific cutting force change, characterized by the rake angle correction factor, that uses the constant  $X$ , is also greater for C/PEEK than for C/PA12.

Based on the obtained constants given in Table 6 and by using equation (3), the specific cutting force on the feed per revolution (over the range from 0.05 to 0.3 mm) and the rake angle (over the range from  $5^\circ$  to  $25^\circ$ ) was calculated and is shown in Figure 4 for C/PA12 and in Figure 5 for C/PEEK.

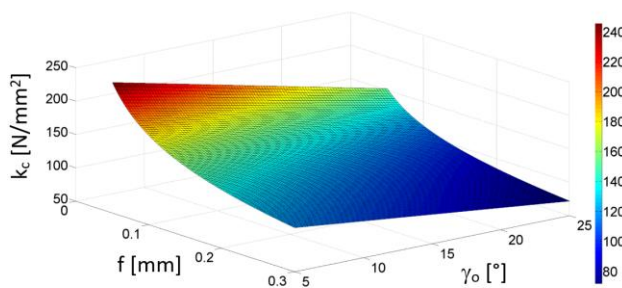


**Figure 4.** Dependence of the specific cutting force on feed per revolution and rake angle for C/PA12

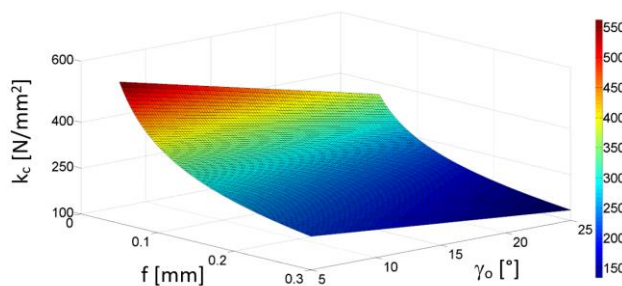


**Figure 5.** Dependence of the specific cutting force on feed per revolution and rake angle for C/PEEK

Figure 6 shows a dependency of the cutting force on the feed per revolution for different rake angles and for both materials. As can be seen there, cutting forces are higher for C/PEEK than for C/PA12 in all cases.

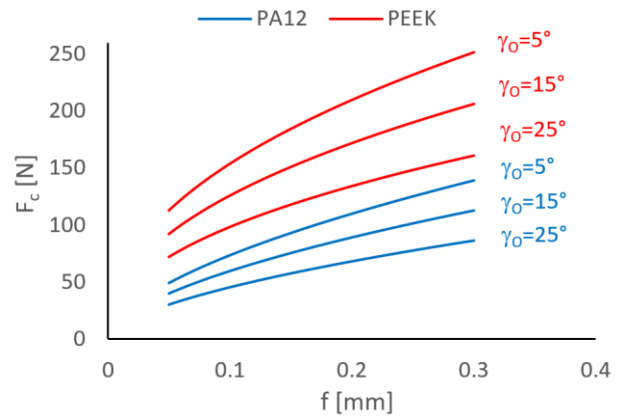


**Figure 6.** Dependence of the cutting force on the feed per revolution for different rake angles and for both materials

### 3.3 Accuracy of the proposed mathematical model

In this part, the cutting force values calculated using the proposed mathematical model, see equation (4), were compared with the experimental cutting force values. To determine it, a paired  $t$ -test was performed. Its results are presented in Table 7.

Material	Mean	StDev	SE Mean	T-Value	p-Value
C/PA12	0.15	6.77	1.24	0.12	0.901
C/PEEK	-0.09	19.26	3.58	-0.02	0.980

**Table 7.** Estimation for paired difference and test statistics

Since the  $p$ -value of both workpiece materials was much higher than the confidence level  $\alpha = 0.05$ , the null hypothesis cannot be rejected and, therefore, it can be stated that for both materials there was not a statistically significant difference between the experimental and calculated cutting force values.

## 4 CONCLUSIONS

In this paper, a cutting force model for orthogonal turning of two widely used types of composite materials, namely C/PA12 and C/PEEK, was proposed. The model was set based on the experimental determination of the effect of feed per revolution, cutting speed and different cutting tool geometry (rake angle) on cutting forces. Uncoated cutting tool inserts of a triangular shape made of sintered carbide were used for experimental force measurements. The key conclusions are summarised as follows:

The key conclusions are summarised as follows:

- Since in all cases the feed force oscillated a lot and the passive force was almost zero, a mathematical model was created only for the cutting force.
- The effect of the feed per revolution and the rake angle on the cutting force is statistically significant for both materials. On the other hand, the effect of the cutting speed on the cutting force is statistically insignificant for both materials.
- A mathematical model of the cutting force with the impact of the feed per revolution as well as the rake angle was developed and based on the experimental data all the constants needed for the model were found.
- A comparison of the calculated and experimental values of the cutting forces showed that there was no statistically significant difference between them.

## ACKNOWLEDGMENTS

The authors would like to acknowledge funding support from the Czech Ministry of Education, Youth and Sports under the project CZ.02.1.01/0.0/0.0/16\_026/0008404 "Machine Tools and Precision Engineering" financed by the OP RDE (ERDF). The project is also co-financed by the European Union.

## REFERENCES

- [Abena 2015] Abena, A., Soo, S. L. and Essa, K. A Finite Element Simulation for Orthogonal Cutting of UD-CFRP Incorporating a Novel Fibre-matrix Interface Model. *Procedia CIRP*, vol. 31, pp. 539–544, 2015.
- [Chang 2006] Chang, C.-S. Turning of glass–fiber reinforced plastics materials with chamfered main cutting edge carbide tools. *Journal of Materials Processing Technology*, vol. 180, no. 1, pp. 117–129, 2006.
- [Chen 2017] Chen, L., Zhang, K., Cheng, H. and Meng, Q. A cutting force predicting model in orthogonal machining of unidirectional CFRP for entire range of fiber orientation. *The International Journal of Advanced Manufacturing Technology*, vol. 89, no. 1–4, pp. 833–846, 2017.
- [Davim 2007a] Davim, J. P. and Mata, F. A comparative evaluation of the turning of reinforced and unreinforced polyamide. *The International Journal of Advanced Manufacturing Technology*, vol. 33, no. 9, pp. 911–914, 2007.
- [Davim 2007b] Davim, J. P. and Mata, F. New machinability study of glass fibre reinforced plastics using polycrystalline diamond and cemented carbide (K15) tools. *Materials & Design*, vol. 28, no. 3, pp. 1050–1054, 2007.
- [Davim 2009] Davim, J. P., Silva, L. R., Festas, A. and Abrão, A. M. Machinability study on precision turning of PA66 polyamide with and without glass fiber reinforcing. *Materials & Design*, vol. 30, no. 2, pp. 228–234, 2009.
- [Davim 2010] Davim, J. P. et al. *Composite Machining*. ISTE London, ISBN 978-1-84821-170-4, 2010.
- [Degner 2015] Degner, W. and Lutze H. *Spanende Formung: Theorie, Berechnung, Richtwerte*. München: Carl Hanser Verlag GmbH & Co. KG, 2015. ISBN 978-3-446-44544-4.
- [Işık 2011] Işık, B. and Altan, E. Cutting Forces in Orthogonal Turning of Unidirectional Glass Fibre Reinforced Plastic Composites. *Advanced Composites Letters*, vol. 20, no. 1, 2011.
- [Kovalčík 2020] Kovalčík, J., Zeman, P., Holešovský, F., Mádl, J. and Kučerová, L. Cutting force modelling with effects of cutting tool geometry and tool wear in milling of DIN C45 steel. *MM Science Journal*, pp. 3784–3793, 2020.
- [Kumar 2014] Kumar, K. V., Sait, A. N. and Panneerselvam, K. Machinability study of hybrid-polymer composite pipe using response surface methodology and genetic algorithm. *Journal of Sandwich Structures and Materials*, vol. 16, no. 4, pp. 418–439, 2014.
- [Kumar 2015] Kumar, S., Gupta, M. and Satsangi, P. S. Multiple-response optimization of cutting forces in turning of UD-GFRP composite using Distance-Based Pareto Genetic Algorithm approach. *Engineering Science and Technology, an International Journal*, vol. 18, no. 4, pp. 680–695, 2015.
- [Mahdi 2001] Mahdi, M. and Zhang, L. A finite element model for the orthogonal cutting of fiber-reinforced composite materials. *Journal of Materials Processing Technology*, vol. 113, no. 1, pp. 373–377, 2001.
- [Mašek 2021] Mašek, P., Zeman, P., Kolář, P. Cutting temperature measurement in turning of thermoplastic composites using a tool-work thermocouple. *The International Journal of Advanced Manufacturing Technology*, vol. 116, pp. 3163–3178, 2021.
- [Ntziantzias 2011] Ntziantzias, I., Kechagias, J., Fountas, N., Maropoulos, S. and Vaxevanidis, N. M. A CUTTING FORCE MODEL IN TURNING OF GLASS FIBER REINFORCED POLYMER COMPOSITE. *International Conference on Economic Engineering and Manufacturing Systems*, 2011.
- [Özden 2021] Özden, G., Öteyaka, M. Ö. and Cabrera, F. M. Modeling of cutting parameters in turning of PEEK composite using artificial neural networks and adaptive-neural fuzzy inference systems. *Journal of Thermoplastic Composite Materials*, 2021.
- [Roy 2014] Roy, Y. A., Gobivel, K., Vijay Sekar, K. S. and Suresh Kumar, S. *High Speed Turning of Carbon Fiber – Epoxy Composite Material*. Vellore, 2014.
- [Santhanakrishnan 1992] Santhanakrishnan, G., Krishnamurthy, R. and Malhotra, S. K. Investigation into the machining of carbon-fibre-reinforced plastics with cemented carbides. *Journal of Materials Processing Technology*, vol. 30, no. 3, pp. 263–275, 1992.
- [Sauer 2020] Sauer, K., Hertel, M., Fickert, S., Witt, M. and Putz, M. Cutting parameter study of CFRP machining by turning and turn-milling. *Procedia CIRP*, vol. 88, pp. 457–461, 2020.
- [Takeyama 1988] Takeyama, H. and Iijima, N. Machinability of Glassfiber Reinforced Plastics and Application of Ultrasonic Machining. *CIRP Annals*, vol. 37, no. 1, pp. 93–96, 1988.
- [Tschatsch 2009] Tschatsch, H. *Applied Machining Technology*. Berlin, Germany: Springer, 2009. ISBN 978-3-642-01006-4.
- [Wang 1995] Wang, D. H., Ramulu, M. and Arola, D. Orthogonal cutting mechanisms of graphite/epoxy composite. Part II: Multi-directional laminate. *International Journal of Machine Tools and Manufacture*, vol. 35, no. 12, pp. 1639–1648, 1995.

## CONTACTS:

Ing. Jaroslav Kovalcik, Ph.D.

Department of Production Machines and Equipment, Faculty of Mechanical Engineering, Czech Technical University in Prague  
Horska 3, 128 00 Prague 2, Czech Republic

+420 221 990 976, j.kovalcik@rcmt.cvut.cz, www.rcmt.cvut.cz